Comparative Biochemistry and Physiology, Part A 250 (2020) 110781

Contents lists available at ScienceDirect

Comparative Biochemistry and Physiology, Part A

journal homepage: www.elsevier.com/locate/cbpa

Interactive effects of temperature and hypoxia on diffusive water flux and oxygen uptake rate in the tidepool sculpin, *Oligocottus maculosus*

Derek A. Somo*, John O. Onukwufor[1], Chris M. Wood, Jeffrey G. Richards

Department of Zoology, The University of British Columbia, Vancouver, BC V6T 1Z4, Canada

ARTICLE INFO

Keywords:
Temperature
Hypoxia
Osmorespiratory compromise
Water flux
Fish

ABSTRACT

The osmorespiratory compromise hypothesis posits that respiratory epithelial characteristics and physiological regulatory mechanisms which promote gas permeability also increase permeability to ions and water. The hypothesis therefore predicts that physiological responses which increase effective gas permeability will result in increased effective ion and water permeabilities. Though analyses of water and gas effective permeabilities using high temperature have generally supported the hypothesis, water permeability responses to hypoxia remain equivocal and the combination of high temperature and hypoxia untested. We measured diffusive water flux (DWF) and oxygen uptake rate ($\dot{M}o_2$) in response to acute temperature change, hypoxia, and the combination of high temperature and hypoxia in a hypoxia-tolerant intertidal fish, the tidepool sculpin (*Oligocottus maculosus*). In support of the osmorespiratory compromise hypothesis, $\dot{M}o_2$ and DWF increased with temperature. In contrast, DWF decreased with hypoxia at a constant temperature, a result consistent with previously observed decoupling of water and gas effective permeabilities during hypoxia exposure in some hypoxia tolerant fishes. However, DWF levels during simultaneous high temperature and hypoxia exposure were not different from fish exposed to high temperature in normoxia, possibly suggesting a failure of the mechanism responsible for downregulating DWF in hypoxia. These results, together with time-course analysis of hypoxia exposure and normoxic recovery, suggest that tidepool sculpins actively downregulate effective water permeability in hypoxia but the mechanism fails with multi-stressor exposure. Future investigations of the mechanistic basis of the regulation of gill permeability will be key to understanding the role of this regulatory ability in the persistence of this species in the dynamic intertidal environment.

1. Introduction

The osmorespiratory compromise hypothesis states that gill characteristics and physiological regulatory mechanisms which increase respiratory gas exchange come at the cost of greater osmoregulatory deficit (Randall et al., 1972; Nilsson, 2007). This trade-off is thought to be a consequence of gills having high surface area, thin epithelia, and constant exposure to the external environment (Randall et al., 1972; Nilsson, 2007). These characteristics, which promote gas conductance across the gill, may also increase the conductance and fluxes of ions and water through this organ (Randall et al., 1972; Nilsson, 2007). Marine teleosts are hyposmotic to seawater, so they tend to gain ions and lose water to the environment. Fish must expend energy to counter these fluxes and maintain osmotic balance (Evans et al., 2005).

The respiratory demands of fish are dynamic, and it is well known that the effective permeability of the gill, defined by functional surface area, diffusion distance, and epithelial permeability, can change with increasing demand for oxygen uptake, as observed during exercise, increasing temperature, or hypoxia exposure (Booth, 1979; Farrell et al., 1980; Soivio and Tuurala, 1981; Randall and Daxboeck, 1984). The osmorespiratory compromise posits that changes in effective permeabilities for oxygen, ions, and water are coupled, so it predicts that an increase in effective permeability to oxygen will lead to increased fluxes of ions and water. Although many studies have examined the effects of changes in effective oxygen permeability on ion fluxes, fewer have focused on changes in water permeability, a key factor in whole-animal osmoregulation (Evans et al., 2005). Studies of changes in water permeability with acute exercise (Hofmann and Butler, 1979; Stevens, 1972; Wood and Randall, 1973; Onukwufor and Wood, 2018) and acute temperature change (Evans, 1969; Isaia, 1972; Motais and Isaia, 1972; Loretz, 1979; Giacomin et al., 2017; Onukwufor and Wood, 2020) generally support the prediction that oxygen and water fluxes change in

* Corresponding author.
E-mail address: somo@zoology.ubc.ca (D.A. Somo).
[1] Present address: Department of Anesthesiology and Perioperative Medicine, University of Rochester Medical Center, Rochester, NY, USA 14642.

https://doi.org/10.1016/j.cbpa.2020.110781
Received 23 January 2020; Received in revised form 31 July 2020; Accepted 31 July 2020
Available online 05 August 2020
1095-6433/

a coupled manner. However, chronic exercise appears to result in a decrease in ionic permeability despite increases in effective oxygen permeability (Wood and Randall, 1973; Gonzalez and McDonald, 1992, 1994; Postlethwaite and McDonald, 1995; Robertson et al., 2015). These results suggest that fish possess regulatory mechanisms that can decouple oxygen and osmotic permeability.

Though acute hypoxia exposure elicits similar increases in effective oxygen permeability as seen in acute exercise and high temperature exposure (Booth, 1979; Soivio and Tuurala, 1981; Randall and Daxboeck, 1984; Nilsson, 2007), relationships between oxygen uptake rate ($\dot{M}o_2$) and diffusive water flux (DWF) with acute hypoxia exposure are more equivocal. Consistent with the osmorespiratory compromise, DWF increases during hypoxia exposure in goldfish (Loretz, 1979) and rainbow trout (Onukwufor and Wood, 2018). In contrast, Wood et al. (2009) observed a decrease in DWF in the Amazonian oscar despite an increase in O_2 transfer factor during hypoxia (Scott et al., 2008). Similarly, DWF decreases during acute hypoxia exposure in freshwater-acclimated Atlantic killifish and remains depressed for at least 3 h during normoxic recovery, and seawater-acclimated fish show no change in DWF with hypoxia despite increases in ventilation (Wood et al., 2019). These results suggest that, in hypoxia tolerant fishes, effective oxygen and water permeabilities are decoupled during hypoxia exposure (Matey et al., 2011).

To our knowledge, no measurements of the combined effects of hypoxia and high temperature on effective osmorespiratory permeabilities have been made, so how these stressors may interact to affect gas, water, and ion exchange is unknown. Hyperoxia, which can co-occur with high temperature in water with high photosynthetic activity (Richards, 2011), did not significantly alter the stimulatory effect of high temperature exposure on DWF in dogfish (*Squalus acanthias suckleyi*) (Giacomin et al., 2017), which could suggest that temperature effects dominate over O_2 effects in determining effective gill water permeability. Given that high temperature often co-occurs with hypoxia in aquatic environments (Diaz and Breitburg, 2009) and the potentially conflicting effects of these stressors individually on $\dot{M}o_2$ and DWF discussed above, there is a need to understand how these stressors interact and affect osmorespiratory balance.

In this study we investigated the effects of temperature, hypoxia, combined high temperature and hypoxia, as well as duration of hypoxia exposure and normoxic recovery on $\dot{M}o_2$ and DWF in the tidepool sculpin (*Oligocottus maculosus*). The tidepool sculpin is found along the northwest coast of North America from Northern California to Alaska, and as its common name implies, it preferentially occupies tidepools (Froese and Pauly, 2007). Tidepools are highly dynamic environments, and temperature and oxygen vary dramatically and regularly in these pools over diurnal timescales (Richards, 2011). Unsurprisingly, tidepool sculpins are among the most hypoxia- and temperature-tolerant sculpins studied (Mandic et al., 2013Mandic et al., 2009b, D. Somo unpublished data).

Using tidepool sculpins, we addressed three objectives. First, we tested the hypothesis that exposure to an acute change in temperature will lead to qualitatively coupled changes in effective oxygen and water permeabilities. Essentially, we are positing that the classic osmorespiratory compromise hypothesis applies to fish when they are exposed to an acute change in temperature. Second, we tested the hypothesis that, during hypoxia exposure in hypoxia tolerant fishes, effective water permeability is reduced through a non-passive, Po_2-dependent mechanism. The reduction in effective water permeability uncouples water and gas permeabilities during hypoxia exposure. Based on these hypotheses, we predicted DWF and $\dot{M}o_2$ would vary directly with acute temperature change. In contrast, in hypoxia, we predicted that DWF would not increase, irrespective of the length of hypoxia exposure, and would lag $\dot{M}o_2$ during normoxic recovery. Our final objective was to investigate the combined effects of hypoxia and high temperature on effective gas and water coupling.

2. Methods

2.1. Animal collection and housing

Tidepool sculpins (*O. maculosus*) (mass = 3.4 ± 0.9 g, avg. ± sd) were collected by dipnet and minnow trap near Bamfield Marine Sciences Centre (BMSC), Bamfield, British Columbia, Canada (48.8355°N, 125.1355°W) under Fisheries and Oceans Canada scientific licence XR-239-2017. Fish were transported to a recirculating seawater system in the aquatics facility at The University of British Columbia, Vancouver, British Columbia, Canada and held for at least 2 months prior to experiments. The system water was maintained at 12.5 ± 0.5 °C, 35‰ salinity, and > 95% atmospheric oxygen saturation, with a 12 h:12 h light:dark photoperiod. During holding fish were fed ad libitum 3 times per week with commercially purchased blood worms and spirulina-loaded brine shrimp (Hikari Sales USA, Hayward, CA, USA). Fish were recovered for at least 3 days, including a feeding day, following each experimental trial before use in subsequent trials. All experiments were carried out under approved animal use protocols at BMSC and The University of British Columbia (BSMC AUP RS-17-11, UBC AUP A13–0309).

2.2. Experimental treatments

Acute hypoxia and temperature effects on DWF and $\dot{M}o_2$ were measured over 40 min of exposure to experimental hypoxic oxygen tensions and acutely increased or decreased temperatures. DWF measurements were restricted to 40 min for technical reasons (see "*Diffusive water flux*" below for details). A temperature of 13 °C and normoxia were considered the control (acclimation) condition. DWF and $\dot{M}o_2$ in tidepool sculpins were measured in normoxia at three temperatures: 6 °C, 13 °C, and 25 °C. Effects of hypoxia on DWF and $\dot{M}o_2$ were measured at 13 °C and two hypoxic oxygen tensions: 4.2 kPa and 2.1 kPa. The interaction of high temperature and hypoxia on DWF and $\dot{M}o_2$ was assessed by measuring DWF and $\dot{M}o_2$ at 25 °C and 2.1 kPa and comparing these data against the hypoxia measurements at 13 °C and 2.1 kPa as well as the normoxic measurements at 25 °C.

To investigate the nature of the regulation of DWF in tidepool sculpins, DWF and $\dot{M}o_2$ were measured in fish exposed to severe hypoxia (2.1 kPa) for 40 min or 3 h, as well as in fish recovered for 40 min or 3 h in normoxia following either the 40 min or 3 h severe hypoxia exposure.

2.3. Diffusive water flux

Prior to experiments, fish were fasted for 3 days. The evening before each diffusive water flux measurement a group of 5 fish were placed in 1 L of 40 μCi tritiated water (^3H_2O, Perkin Elmer, Woodbridge, ON, Canada) in an aerated, covered, black-plastic coated container submerged in a water bath held at 13 °C for overnight equilibration with the radioisotope (minimum 12 h). Following the equilibration period each fish was gently removed from the equilibration bath by dipnet, quickly rinsed with ^3H_2O-free water to remove any ^3H_2O on the body surface of the fish, and placed in a 100-mL container of 35‰ salinity, ^3H_2O-free water at the appropriate experimental temperature and oxygen tension. Immediately after placing the fish in the container, 1 mL of water was sampled at 0 and every 5 min thereafter for the next 60 min. A final 1-mL sample was taken 12 h after the start of each trial when washout was complete. The fish were then weighed and returned to their acclimation tanks for recovery before subsequent trials. The 0–40 min samples were used to calculate diffusive water flux and the 12-h sample was used to calculate the original dose of ^3H_2O in the fish at time 0 (see calculations below). Because the efflux of ^3H_2O from the fish is rapid, all DWF measurements had to be made over the first 40 min after transfer to the ^3H_2O-free container (see Section 2.4.1). For DWF measurements in the longer-term hypoxia and normoxic recovery

experimental treatments, fish were first exposed to the treatment condition (hypoxia) in the ^3H_2O equilibration container so that measurements could be made during the first 40 min after transfer to ^3H_2O-free water. Oxygen tensions were reduced from normoxia to 2.1 kPa or returned to normoxia from hypoxia within 1–2 min. Fish were rapidly transferred from the equilibration container to the ^3H_2O-free experimental treatment container which was already at the target oxygen tension for the final 40 min of exposure.

2.4. Respirometry

$\dot{M}o_2$ was measured using intermittent-flow respirometry. Fish were placed individually in approximately 75-mL glass respirometers, with a respirometer volume-to-fish mass ratio of 20:1. Respirometers were submerged in a water bath held at experimental temperature and oxygen tension. Temperature was controlled using a benchtop temperature regulator (model 1160S, VWR International, Radnor, PA, USA) connected to a water-filled stainless-steel heat-exchange coil submerged in the bath. Oxygen tension of the bath was either kept in equilibrium with atmospheric levels by bubbling air or maintained at target hypoxia levels by manually adjusting nitrogen and air flow rates into the bath. A plastic bubble-wrap covering minimized atmospheric oxygen ingress into the bath in hypoxia trials. Respirometers were connected to flushing pumps which fed water from the bath into the respirometers during flushing periods. Oxygen tension in the water bath was monitored using a handheld dissolved oxygen meter connected to a galvanic oxygen probe (model DO110, Oakton Instruments, Vernon Hills, IL, USA). Oxygen tension was sampled inside respirometers using a fiber-optic fluorescent probe in a stainless-steel housing (FOXY system, Ocean Optics, Dunedin, FL, USA) and recorded every 15 s using Ocean Optics' NeoFox software. Magnetic stir bars below a false bottom mixed water inside the respirometers. Black plastic was placed on top of the water to prevent visual disturbance of the fish. Flushing and closed periods were automated using Aquaresp v 3.0 software (AquaResp.com) to power flush pumps through a USB power switch (model Cleware 1 USB-SwitchC IEC 16A Product no.:24–1, Cleware GmbH, Germany). Flushing periods were 360 s, and closed periods were a minimum 360 s in order to ensure a minimum 300 s linear decline in oxygen tension. Fish were weighed immediately following the respirometry period.

2.4.1. Analytical techniques and calculations: Diffusive water flux

Diffusive water efflux analytical methods followed Onukwufor and Wood (2018). Briefly, the concentration of ^3H_2O in water samples was analyzed using a scintillation counter (LS6500, Beckman Coulter, Fullerton, CA, USA). Two ml of Optiphase 3 fluor (Perkin-Elmer, Wellesley, MA, USA) was added to the 1-mL water sample. Internal standardization tests demonstrated that quenching was constant, so no correction was necessary.

The rate constant of ^3H_2O efflux, representing the unidirectional efflux of water expressed as a decimal fraction of the total body water pool per hour (h^{-1}), was calculated by determining the rate of decline in the ^3H_2O in the fish, which is known to be approximately exponential with time (Evans, 1967):

$$k = \frac{\ln CPM_1 - \ln CPM_2}{time_1 - time_2} \quad (1)$$

where k is the rate constant of efflux (in h^{-1}), CPM_1 is the total ^3H_2O radioactivity (in cpm) in the fish at $time_1$ (in h), and CPM_2 is the total ^3H_2O radioactivity (in cpm) in the fish at $time_2$ (in h). This relationship was linear over time for all fish until 40 min, after which some departures from linearity occurred, likely due to the tritiated water specific activity becoming high enough in the external compartment that significant back-flux occurred. Therefore k was calculated using the first 40 min of data. The product of k × 100% gives the percentage of body water turned over per hour.

The total amount of radioactivity that had been taken up by the fish during the loading period (CPM_{total}) was estimated after equilibration (12h) from the measured ^3H_2O radioactivity in the 12 h water sample and volume of the water in the container at that time point. From CPM_{total}, the water volume present at each time point, measurements of ^3H_2O radioactivity appearance in the water at each sampling time, and accounting for the radioactivity removed with each water sample, we back-calculated the CPM in the fish at each sampling time point during each efflux experiment. ^3H_2O efflux rates were calculated by regressing the natural logarithm of CPM in the fish against time over the 40 min measurement period to yield the slope k (Eq. 1).

Water efflux rate constants (k) were converted to diffusive water flux rates in mL per h by assuming that the water space is 80% of the body mass of the fish (Holmes and Donaldson, 1969; Isaia, 1984; Olson, 1992):

$$DWF = M * k * 0.8 \quad (2)$$

where DWF is diffusive water flux in mL/h, M is fish body mass in g, k is the rate constant, and 0.8 is the fractional body water pool.

Due to design constraints, the experimental containers used in the DFW experiments allowed fish access to the water surface. Fish could have avoided aquatic hypoxia to an unknown degree by respiring at the surface of the water, which may have affected DWF. This species is known to perform both aquatic surface respiration (ASR) and aerial emersion when exposed to aquatic hypoxia (Mandic et al., 2009a; Yoshiyama et al., 1995) but not to high temperature, at least in the laboratory setting (personal observation, D. Somo). To assess the effect of air access we measured DWF in fish without air access at 25 °C and 2.1 kPa oxygen. Fish were expected to perform the highest frequency of ASR in this condition and therefore air access was expected to most affect DWF. Air access did not affect DWF ($F_{1,10}$ = 1.91, P = 0.2, Supplementary Fig. S1). DWF data obtained from sculpins both with and without air access in the 25 °C and 2.1 kPa oxygen treatment were grouped together in all subsequent analyses.

2.4.2. Analytical techniques and calculations: Oxygen uptake rate

Water oxygen content in respirometers was converted from recorded percent air saturation values to oxygen partial pressure in kPa using local reported barometric pressure measurements at the nearest Department of Environment and Natural Resources Canada weather station (49° 11′ 41” N, 123° 11′ 2” W) and assuming an atmospheric oxygen fraction of 0.2095. Oxygen partial pressure was converted to μmol O_2 using salinity- and temperature-appropriate solubility coefficients from Boutilier et al. (1984) and the volume of the respirometer less the volume of the fish, with an assumed fish density of 1 mL/g. $\dot{M}o_2$ (μmol/h) was calculated from each “closed period” using a minimum of 300 s of the most linear portion of the slope ($R^2 \geq 0.9$) using Labchart Reader v8.1.9 (ADInstruments Inc., Colorado Springs, CO, USA). During the hypoxic trials, oxygen partial pressure in the respirometers when the respirometers were closed to flow started above and dropped below the target level such that the mean oxygen partial pressure equaled the desired experimental level. Oxygen saturation did not vary by more than 1.5% air saturation above or below the desired experimental level. Oxygen saturation in normoxic trials did not fall below 75% air saturation. Measurement trials lasted 40 min to match the time period of the DWF calculations. There were no significant differences in $\dot{M}o_2$ between 0 and 20 min and 20–40 min. Each trial typically yielded 3–4 oxygen consumption rate measurements per individual fish. These were averaged for each fish and the average $\dot{M}o_2$ per fish per h was used in subsequent analyses.

2.4.3. Analytical techniques and calculations: Body mass effects

Body mass is known to affect both $\dot{M}o_2$ and DWF. However, the fish used in this study came from a small size range relative to the adult size range of the species (~ 30% of adult body mass range (Froese and Pauly, 2007), and body mass-metabolic rate scaling relationships are known to vary with temperature in many species of fish (Clarke and

Table 1
Mass by treatment ANCOVA results for each experiment.

Model	$F_{(df\ num,\ df\ denom)}$	*P*
ln(DWF) ~ ln(M) + T	ln(M): $F_{1,16} = 54.3$	ln(M): $P = 1.59 \times 10^{-6}$
	T: $F_{2,16} = 175.7$	T: $P = 1.30 \times 10^{-11}$
$\dot{M}o_2$ ~ M + T	M: $F_{1,14} = 15.6$	M: $P = 0.001$
	T: $F_{2,14} = 11.3$	T: P = 0.001
DWF ~ M + P	M: $F_{1,21} = 45.9$	M: $P = 1.07 \times 10^{-6}$
	P: $F_{2,21} = 5.95$	P: $P = 0.009$
ln($\dot{M}o_2$) ~ M + P	M: $F_{1,15} = 7.53$	M: $P = 0.015$
	P: $F_{2,15} = 44.6$	P: $P = 4.84 \times 10^{-7}$
ln(DWF) ~ M + TP	M: $F_{1,29} = 65.6$	M: $P = 6.21 \times 10^{-9}$
	TP: $F_{3,29} = 86.3$	TP: $P = 1.48 \times 10^{-14}$
ln($\dot{M}o_2$) ~ M + TP	M: $F_{1,18} = 11.9$	M: $P = 0.0029$
	TP: $F_{3,18} = 72.8$	TP: $P = 2.93 \times 10^{-10}$
DWF ~ M + Time	M: $F_{1,52} = 164$	M: $P < 2 \times 10^{-16}$
	Time: $F_{6,52} = 10.0$	Time: $P = 2.49 \times 10^{-7}$
ln($\dot{M}o_2$) ~ M + Time	M: $F_{1,35} = 11.1$	M: $P = 0.0020$
	Time: $F_{6,35} = 23.0$	Time: $P = 8.42 \times 10^{-11}$

M = Body mass, T = Temperature, P = Po_2, TP = Combined Temperature-Po_2, Time = Hypoxia or normoxic recovery timecourse. Response variables and body mass were natural logarithm transformed as necessary to meet assumptions of normality and homoscedasticity of model residuals.

Johnston, 1999), so relationships between body mass and $\dot{M}o_2$ and DWF, and possible interactions between mass and treatment effects were assessed for each experiment by fitting linear models to $\dot{M}o_2$ or DWF data:

$$Y = a + bM + cT + dMT \quad (3.1)$$

$$\ln(Y) = a + bM + cT + dMT \quad (3.2)$$

$$\ln(Y) = a + b\ \ln(M) + cT + d\ \ln(M)T \quad (3.3)$$

where *Y* is either $\dot{M}o_2$ or DWF, *a*, *b*, *c*, and *d* are estimated constants, *M* is body mass in grams, and *T* are treatment effects (e.g. temperature, hypoxia, combined temperature-hypoxia, or time course effects). If model residuals were not normally distributed or homoscedastic, the model was refitted with the natural logarithm of the response *Y* (Eq. 3.2) and, if necessary, the natural logarithm of body mass *M* (Eq. 3.3). Body mass (or ln(Mass)) was a significant term in every relationship (Table 1) but there were no significant interactions between mass and treatment terms. Therefore the $\dot{M}o_2$ or DWF versus mass and treatment effects models were refitted without the interaction term (Table 1) and data were adjusted to the value for a 3.5 g fish (representing the approximate average body mass of fish used in this study) by solving the system of equations for the 3.5 g-adjusted response value and the observed response value (corresponding to Eqs. 3.1–3.3 (without the interaction term), respectively):

$$Y_{3.5g} = Y_{obs} - b(3.5g - M_{obs}) \quad (4.1)$$

$$Y_{3.5g} = Y_{obs} * e^{(b(3.5g - M_{obs}))} \quad (4.2)$$

$$Y_{3.5g} = Y_{obs} * e^{\left(b * \ln\left(\frac{3.5g}{M_{obs}}\right)\right)} \quad (4.3)$$

where *b* is the slope of the body mass effect from the appropriate model. These adjusted rates were then divided by 3.5 g to obtain a per-gram rate for use in subsequent statistical analyses.

2.4.4. Analytical techniques and calculations: Temperature sensitivity of oxygen uptake rate and diffusive water flux

Q_{10} values were calculated to describe the temperature sensitivity of $\dot{M}o_2$ and DWF as follows:

$$Q_{10} = \left(\frac{R_2}{R_1}\right)^{\left(\frac{10}{T_2 - T_1}\right)} \quad (5)$$

where R_2 and R_1 are the observed body mass-adjusted rates at temperatures T_2 (°C) and T_1 (°C), respectively.

2.5. Statistical analysis

All statistical analyses were performed in R v 4.0.0 "Arbor Day" (R Core Team, 2020). The effects of acute hypoxia exposure, acute temperature change, the combination of high temperature and hypoxia, and length of hypoxia exposure and recovery time on mass-specific $\dot{M}o_2$ and DWF were analyzed using ANOVA unless the assumptions of normality and homoscedasticity of the model residuals were not met. In such case a Kruskal-Wallis analysis of variance on ranks was used. All data are expressed as mean ± 95% SEM (N). Significant treatment effects were followed by Tukey's HSD post hoc tests with $p < 0.05$ for significant ANOVA effects and by Dunn's test of multiple comparisons with $p < 0.05$ following significant Kruskal-Wallis ANOVA on ranks effects.

To account for Type I error inflation due to use of some data (e.g. control data at 13 °C and 21.2 kPa) in multiple hypothesis tests, *p*-values obtained from all significant hypothesis tests were adjusted using a Benjamini-Hochberg False Discovery Rate correction. None of the adjusted p-values were greater than 0.05, so the unadjusted *p* values and associated hypothesis test statistics are reported below.

3. Results

3.1. Effects of temperature on $\dot{M}o_2$ and diffusive water flux

In normoxia, both $\dot{M}o_2$ and DWF increased with temperature ($\dot{M}o_2$: $F_{2,15} = 12.24$, $P < < 0.001$; DWF: $F_{2,17} = 192.7$, $P < < 0.001$; Fig. 1A,B). The Q_{10} values of $\dot{M}o_2$ and DWF were higher between 6 and 13 °C than between 13 and 25 °C, and the Q_{10} values for DWF were consistently higher than for $\dot{M}o_2$ over both temperature ranges (Fig. 1A,B).

3.2. Effects of hypoxia on $\dot{M}o_2$ and diffusive water flux

At 13 °C, both $\dot{M}o_2$ and DWF decreased with decreasing oxygen tension ($\dot{M}o_2$: $F_{2,16} = 48.15$, $P = 1.70 \times 10^{-7}$; DWF: $F_{2,21} = 6.09$, $P = 0.008$; Fig. 2A,B). Though $\dot{M}o_2$ fell between 4.2 kPa and 2.1 kPa (Fig. 2A), DWF did not decrease further in the more hypoxic condition (Fig. 2B).

3.3. Effects of combined temperature and oxygen treatments on $\dot{M}o_2$ and diffusive water flux

$\dot{M}o_2$ fell in severe hypoxia (2.1 kPa) at both 13 °C and 25 °C to the same extent (Tukey post-hoc comparison: $P = 0.38$), with no statistical difference in $\dot{M}o_2$ between 25 °C than 13 °C in normoxia (Tukey post-hoc comparison: $P = 0.071$) (ANOVA: $F_{3,19} = 76.84$, $P = 8.28 \times 10^{-11}$, Fig. 3A). The effect of severe hypoxia on DWF depended on temperature ($F_{3,30} = 89.25$, $P = 4.78 \times 10^{-15}$, Fig. 3B). DWF decreased in hypoxia at 13 °C compared to normoxia and did not differ between hypoxia and normoxia at 25 °C (Fig. 3B).

3.4. Effects of duration of hypoxia exposure and recovery on $\dot{M}o_2$ and diffusive water flux

$\dot{M}o_2$ in hypoxia fell below control values in the first 40 min and third hour of exposure but recovered to control values within 40 min once fish were placed in normoxic water (Kruskal-Wallis H = 28.85, df = 6, $P = 6.51 \times 10^{-5}$; Fig. 4A).

DWF declined within the first 40 min of severe hypoxia (2.1 kPa) exposure and similarly fell after 3 h of hypoxia exposure ($F_{6,52} = 11.24$, $P = 5.20 \times 10^{-8}$, Fig. 4B). DWF was marginally depressed below control values during the first 40 min of recovery from 1 h of severe hypoxia exposure (Tukey post-hoc comparison: $P = 0.10$, Fig. 4B) and

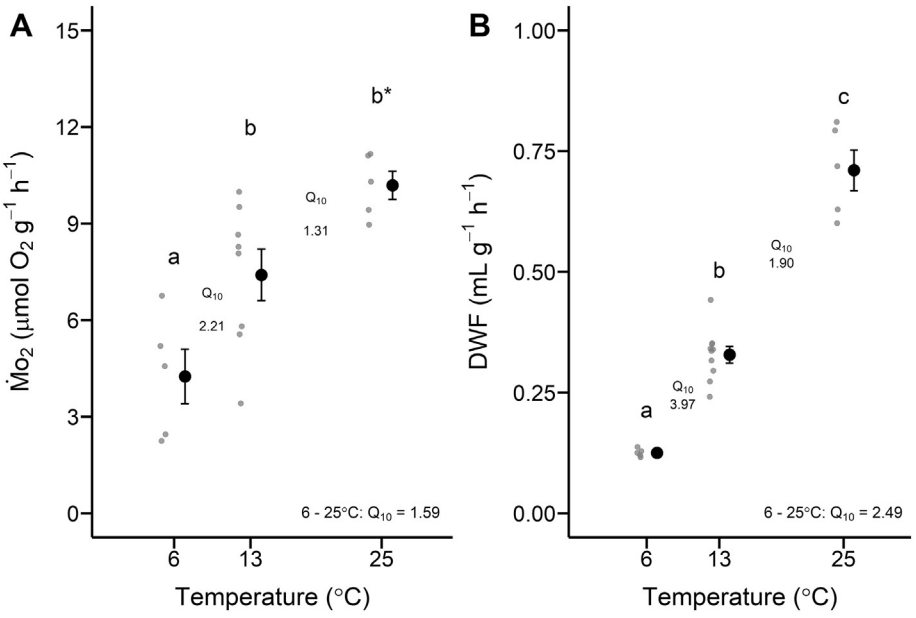

Fig. 1. Effects of acute temperature change in normoxia on (A) $\dot{M}o_2$ and (B) DWF. Grey circles are raw data. Black circles are means and error bars are standard error of the mean. Within each plot, different letters represent significant differences between means. Numbers between data are Q_{10} values, and an overall Q_{10} for the full experimental temperature range is given in the bottom right of each graph. $^*P = 0.05$ for Tukey post-hoc comparison of $\dot{M}o_2$ at 13 °C and 25 °C.

fell significantly below both control and 40-min hypoxia exposure levels by 3 h of recovery (Fig. 4B). In contrast, following a 3-h exposure to severe hypoxia, DWF had recovered to near-control values within an hour of normoxic recovery (Fig. 4B).

4. Discussion

4.1. DWF and $\dot{M}o_2$ both increase with increasing temperature

The effect of temperature on DWF and $\dot{M}o_2$ was consistent with the osmorespiratory compromise hypothesis. $\dot{M}o_2$ and DWF both increased with temperature, suggesting that increased oxygen uptake at higher temperature was accompanied by increased effective water permeability. Our observed responses to acute temperature change are generally consistent with previous reports of the effect of acute temperature change on $\dot{M}o_2$ (Clarke, 2017) and DWF (Evans, 1969; Motais and Isaia, 1972; Loretz, 1979; Giacomin et al., 2017; Onukwufor and Wood, 2018, 2020) in fishes. Likewise, the Q_{10} values for $\dot{M}o_2$ (Fig. 1A) and DWF (Fig. 1B) were well within previously reported ranges (Evans, 1969; Isaia, 1972; Motais and Isaia, 1972; Loretz, 1979; Giacomin et al., 2017; Onukwufor and Wood, 2018, 2020). The higher Q_{10} values in $\dot{M}o_2$ and DWF at the lower temperature range have been observed in previous studies (e.g. Giacomin et al., 2017; Onukwufor and Wood, 2018, 2020). Decreasing Q_{10} values at higher temperatures within an organism's thermal performance range likely reflect the deceleration towards a peak (optimum) rate characteristic of many thermal performance curves (TPC) (Sinclair et al., 2016). Additional measurements across the full acute temperature tolerance range to determine whether both $\dot{M}o_2$ and DWF exhibit the common left-skewed bell-shaped TPC or diverge in shape could provide further evidence whether or not there exists a shared temperature-based regulatory mechanism for these traits.

The consistently higher Q_{10} values for DWF relative to $\dot{M}o_2$ may reflect the involvement of aquaporin protein channels in the former. Aquaporin involvement in water permeability in fishes may be a key component of the molecular basis of fish osmoregulation, but aquaporins are poorly studied in fishes in general (Madsen et al., 2015). There is evidence of the involvement of aquaporin protein AQP3 in DWF changes in the gills of freshwater-acclimated Atlantic killifish (Ruhr et al., 2020). Biologically-mediated processes, such as facilitated

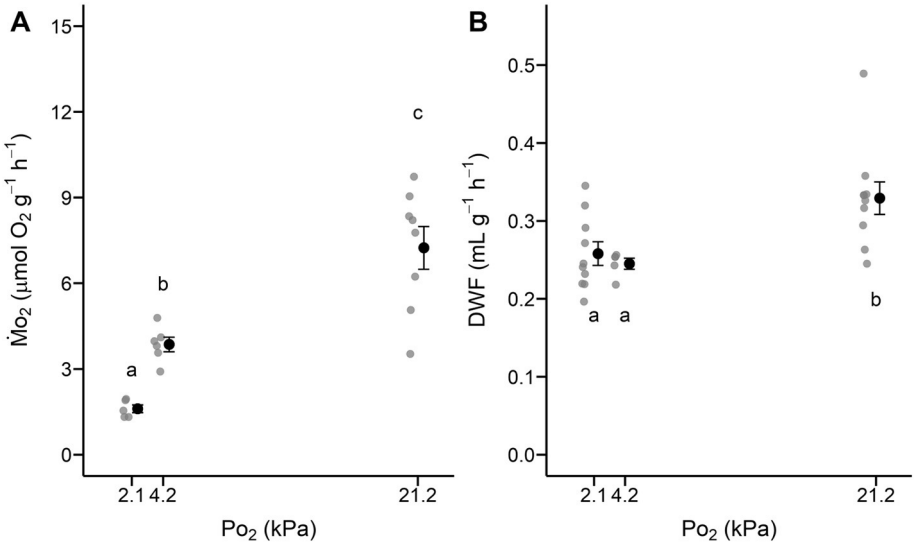

Fig. 2. Acute hypoxia exposure effects at 13 °C on (A) $\dot{M}o_2$ and (B) DWF. Symbols and statistical notation are as described in Fig. 1.

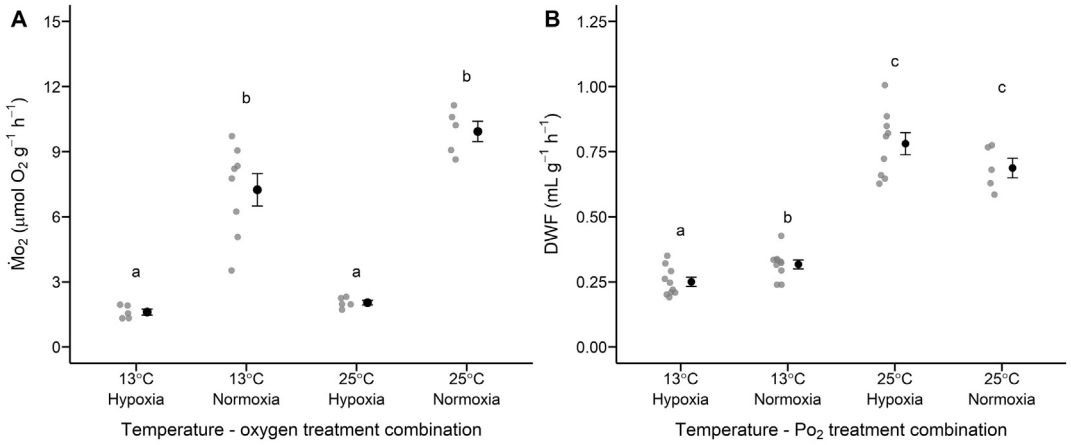

Fig. 3. Effects of acute high temperature (25 °C) exposure, severe hypoxia (2.1 kPa), and combined high temperature and hypoxia on $\dot{M}o_2$ and DWF. Symbols and statistical notation are as described in Fig. 1.

diffusion through protein channels, typically have much higher Q_{10}s than passive processes. Based on the osmorespiratory compromise, we might predict that cardiorespiratory responses to increasing tissue demand for oxygen with increasing temperature, such as increases in functional gill surface area and increasing bulk blood and water flows past the gills, could effect similar changes in the rates of $\dot{M}o_2$ and DWF. If aquaporin proteins play an important role in facilitating DWF at the gill, then an additive or synergistic effect of the thermal sensitivity of aquaporin function to the effects of cardiorespiratory responses to warming could explain the higher thermal sensitivity of DWF compared with $\dot{M}o_2$ (Onukwufor and Wood, 2020). However, $\dot{M}o_2$ and effective oxygen permeability at the gill depends greatly on blood oxygen binding properties (Nikinmaa and Salama, 1998). Fish blood oxygen binding and the effects of temperature are regulated by a complex suite of factors, including the temperature sensitivity of hemoglobin-oxygen binding, the temperature sensitivity of organic phosphate-hemoglobin binding and red cell organic phosphate metabolism, and temperature effects on red cell pH, among others (Nikinmaa, 1990). Together the effects of temperature on these traits, as well as temperature effects on tissue oxygen extraction, venous Po_2, cardiac output, and blood transit through the gills, determine the arterio-venous difference in blood Po_2, which is a key factor setting the effective permeability of the fish to oxygen and ultimately $\dot{M}o_2$. To parse the differences in DWF and $\dot{M}o_2$ temperature sensitivity, future studies should investigate the possible role of aquaporin proteins and their thermal sensitivity in setting the thermal sensitivity of DWF in conjunction with the thermal physiology of in-vivo blood oxygen binding.

4.2. $\dot{M}o_2$ and DWF decrease in hypoxia

Fish exposed to hypoxia typically increase ventilation and functional surface area at the gill (Randall and Daxboeck, 1984; Perry et al., 2009) to maintain the rate of oxygen uptake required to meet demand at the tissues in the face of declining availability of oxygen in the water. The classic osmorespiratory compromise predicts that these physiological responses at the gill not only increase permeability to oxygen but to ions and water as well. DWF does increase with hypoxia exposure in goldfish (Loretz, 1979) and rainbow trout (Onukwufor and Wood, 2018). However, accumulating evidence suggests that some hypoxia-tolerant fishes are able to suppress gill ion and water permeability during hypoxia exposure (Wood et al., 2009, 2019; Matey et al., 2011; Giacomin et al., 2020), despite increases in ventilation (Giacomin et al., 2019; Wood et al., 2019) and oxygen transfer factor (Scott et al., 2008), decoupling the effective permeability of the gill to oxygen from

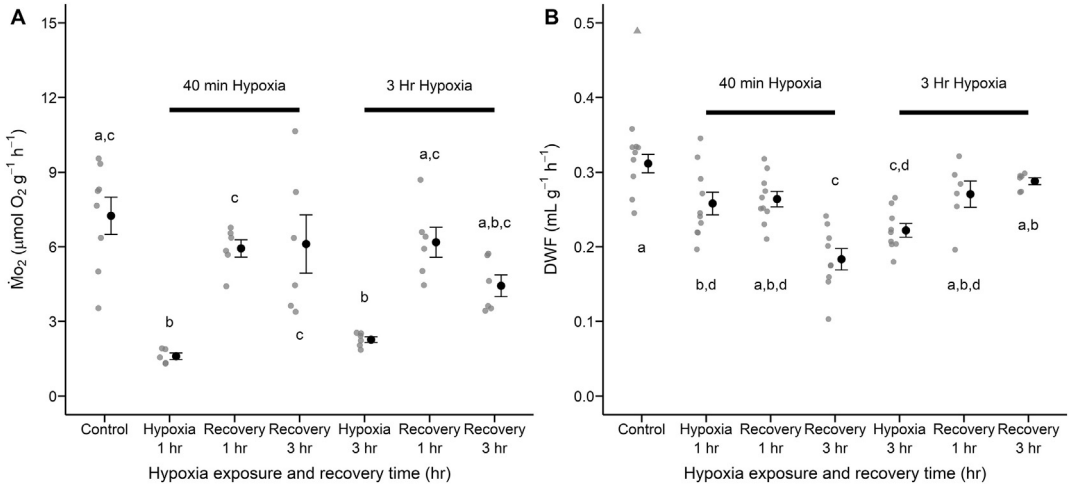

Fig. 4. Effect of duration of hypoxia and normoxic recovery on $\dot{M}o_2$ and DWF. In the hypoxia exposure treatments, fish were exposed to either 40 min or 3 h of severe hypoxia (2.1 kPa O_2). The effect of normoxic recovery duration on $\dot{M}o_2$ and DWF was determined in fish first exposed to 40 min or 3 h of severe hypoxia (2.1 kPa O_2) followed by either 40 min or 3 h of normoxia. The black bars indicate the duration of hypoxia exposure prior to any normoxic recovery period. Grey and black symbols and statistical notation are as described in Fig. 1, except the grey triangle in (B) represents an outlier. Removal of this outlier did not change statistical results so it was retained in the final analysis.

effective permeability to ions and water. In support of the osmorespiratory hypoxic decoupling hypothesis, DWF was equally suppressed at both hypoxic Po_2s in tidepool sculpins despite a progressive decline in $\dot{M}o_2$ (Fig. 2B). Although $\dot{M}o_2$ declined during hypoxia exposure (Fig. 2A), this decline likely does not reflect a decrease in effective oxygen permeability, which is likely elevated in hypoxia, but rather a severe decrease in the Po_2 gradient driving oxygen uptake. Active metabolic suppression could contribute to the observed fall in $\dot{M}o_2$, but based on the proximity of our experimental hypoxic Po_2 and $\dot{M}o_2$ values (Fig. 2A) to the published critical oxygen tension and routine $\dot{M}o_2$ of this species (~ 3.45 kPa and ~ 2.5 μmol O_2 g^{-1} h^{-1}, Mandic et al., 2009b; Sloman et al., 2008) and the large accumulation of lactate during sub-P_{crit} hypoxia exposure in tidepool sculpins compared with closely related species (Speers-Roesch et al., 2013), we believe metabolic suppression is unlikely to explain the decline in $\dot{M}o_2$ in hypoxia. Future studies should investigate the possible role of metabolic suppression in the decoupling of oxygen and osmotic permeabilities during hypoxia exposure in tidepool sculpins and other hypoxia tolerant fishes. Overall, the suppression of DWF during hypoxia exposure in this species likely reflects a biologically-mediated suppression of water permeability during hypoxia exposure.

The decrease of DWF in hypoxia in tidepool sculpins suggests this species may actively suppress DWF, though the mechanism remains unknown. Tidepool sculpins are a hypoxia tolerant species (Mandic et al., 2013, 2009b) that occupies the oxygen- and salinity-variable intertidal environment (Froese and Pauly, 2007). This species may downregulate gill water permeability similar to the Amazonian oscar. Wood et al. (2009) demonstrated a regulated decrease in gill water and ion permeability during hypoxia exposure in Amazonian oscar. These workers proposed that a regulated decrease in the permeability of water and ion channels, coupled with covering of apical crypts in ionocytes by pavement cells, could reduce water and ion fluxes across the gill and therefore reduce energy expended on osmoregulation in hypoxia in Amazonian oscar (Wood et al., 2009). There are however important differences between the oscar and the tidepool sculpin and between freshwater and seawater teleost gills in general that might affect the ability of tidepool sculpins to use “morphological channel arrest” (MCA) as Amazonian oscars do (Wood et al., 2009). The spatial arrangement of single ionocytes surrounded by pavement cells in freshwater fish lamellae (Evans et al., 2005) coupled with a generally low density of ionocytes in oscar (Wood et al., 2009) may facilitate large effects on transcellular ionocyte permeability due to coverage by pavement cells in hypoxia. It is unknown whether pavement cells can cover the apical grooves of the multi-ionocyte complexes characteristic of seawater teleost gills (Evans et al., 2005). DWF remained depressed and even decreased further after 3 h of normoxic recovery following 1 h of hypoxia exposure (Fig. 4B). A similar prolonged depression of DWF during normoxic recovery was seen in freshwater-acclimated Atlantic killifish (Wood et al., 2019) and down-regulation of aquaporin AQP3 protein abundance in the gills has been implicated in this response (Ruhr et al., 2020). Intriguingly, in tidepool sculpins, although 3 h of hypoxia exposure appeared to maximally depress DWF, within an hour of normoxic recovery following 3 h of hypoxia DWF did not differ from control values (Fig. 4B), similar to observations in the oscar (Wood et al., 2009). These observations suggest potentially complex regulation of gill water permeability following prolonged hypoxia exposure in tidepool sculpins and other hypoxia tolerant species.

4.3. The downregulation of DWF in hypoxia in tidepool sculpins is temperature-dependent

Though DWF decreases in hypoxia in tidepool sculpins at 13 °C, DWF increases substantially when tidepool sculpins are acutely exposed to 25 °C, irrespective of hypoxia or normoxia exposure (Fig. 3B). To our knowledge these are the first data published on the combined effect of acute hypoxia and high temperature on DWF in a teleost fish. Tidepool sculpins may experience both 13 °C and 25 °C during a single tidal cycle, and in certain circumstances can experience hypoxia at these high temperatures. The potential failure of the regulatory mechanism lowering DWF in cool, hypoxic water could suggest that fish experiencing high temperature and hypoxia not only must take up more O_2 to meet the temperature-induced increase in metabolic demand while O_2 availability is constrained, but more of the oxygen taken up must be used to maintain osmotic homeostasis. The temperature-dependence of important regulatory mechanisms like DWF regulation could contribute to the synergistic and insidious effects of multi-stressor exposures like high temperature and hypoxia on organismal performance. Future investigations of the failure of biological regulation under multi-stressor exposure is an important area for advancing our understanding and predictive capacity for organismal responses to the multifaceted environmental changes expected with climate change.

4.4. The skin could play a role in osmorespiratory regulation in tidepool sculpins

Though the gill is typically the site where most gas uptake/excretion and ion regulation occurs, the skin could contribute importantly to the whole-organism osmorespiratory responses we observed in this study. The skin is known to contribute to osmorespiratory exchange in many intertidal fishes (Martin and Bridges, 1999; LeBlanc et al., 2010). In tidepool sculpins the skin may contribute up to ~20% of ammonia and urea excretion (Wright et al., 1995). Glover et al. (2013) point out that partitioning osmoregulation between the gills and skin could be advantageous in alleviating the osmorespiratory compromise by spatially separating respiratory and osmoregulatory processes, particularly during exposure to stressful conditions. Importantly, understanding whether the regulation of skin effective permeability in hypoxia-tolerant fishes like the tidepool sculpin contributes to overall osmorespiratory regulation during stress exposure could be important in understanding possible threshold effects of multiple stressor exposures. For instance, increasing skin perfusion to supplement oxygen uptake at the gill during combined high temperature and hypoxia exposure could lead to dramatic changes in ionic or osmotic fluxes like that observed in our study (Fig. 3B). Future studies should investigate the possible contribution of skin to osmorespiratory responses to environmental stressors and the potential tradeoffs involved in recruiting skin for osmotic or respiratory regulation.

5. Conclusions

In support of the osmorespiratory compromise hypothesis, DWF and $\dot{M}o_2$ both varied directly with temperature in normoxia in tidepool sculpins. In contrast, both $\dot{M}o_2$ and DWF fell in hypoxia, as has been reported in a number of other hypoxia-tolerant fish species. This result adds to a growing body of evidence supporting a hypoxic osmorespiratory decoupling in hypoxia tolerant species. Based on our analysis of the effects of duration of hypoxia exposure and normoxic recovery, the decline in DWF in hypoxia is likely a physiological response under complex regulation. However, it is unclear what mechanism underlies the decline in DWF in hypoxia observed here and whether changes in gill morphology in hypoxia contribute to this response in tidepool sculpins as in Amazonian oscar, or whether aquaporins are involved as in the Atlantic killifish. Combined changes in effective osmotic and oxygen permeabilities following prolonged hypoxia exposure could affect the cost of oxygen uptake from an osmorespiratory perspective and should be investigated along with morphological responses at the gill. The failure of downregulation of DWF in hypoxia at high temperature raises important questions about biological regulation under multi-stressor conditions. These questions are not only of interest from ecological and evolutionary perspectives but are compelling in the context of current and projected changes in multiple environmental parameters with climate change.

Supplementary data to this article can be found online at https://doi.org/10.1016/j.cbpa.2020.110781.

Declaration of Competing Interest

The authors declare that they have no known competing financial interests or personal relationships that could have appeared to influence the work reported in this paper.

Acknowledgements

This work was supported by Natural Sciences and Engineering Research Council of Canada Discovery Grants to JGR [F14-04709] and CMW [RGPIN 2017-03843]. DAS is supported by The University of British Columbia Four Year Fellowship. We thank the staff at Bamfield Marine Sciences Centre for technical and logistical support of fish collections, especially Eric Clelland.

References

Booth, J.H., 1979. The effects of oxygen supply, epinephrine, and acetylcholine on the distribution of blood flow in trout gills. J. Exp. Biol. 83, 31–39.
Boutilier, R.G., Heming, T.A., Iwama, G.K., 1984. Appendix: Physicochemical parameters for use in fish respiratory physiology. In: Hoar, W.S., Randall, D.J. (Eds.), Fish Physiology: Gills - Anatomy, Gas Transfer, and Acid-Base Regulation. Part A 10. Academic Press, London, pp. 403–430.
Clarke, A., 2017. Principles of Thermal Ecology. Oxford University Press, Oxford.
Clarke, A., Johnston, N.M., 1999. Scaling of metabolic rate with body mass and temperature in teleost fish. J. Anim. Ecol. 68, 893–905.
Diaz, R.J., Breitburg, D.L., 2009. The hypoxic environment. In: Richards, J.G., Farrell, A.P., Brauner, C.J. (Eds.), Fish Physiology: Hypoxia. 27. Academic Press, London, pp. 1–23.
Evans, D.H., 1967. Sodium, chloride and water balance of the intertidal teleost, Xiphister atropurpureus. I. Regulation of plasma concentration and body water content. J. Exp. Biol. 47, 513–517.
Evans, D.H., 1969. Studies on the permeability to water of selected marine, freshwater and euryhaline teleosts. J. Exp. Biol. 50, 689–703.
Evans, D.H., Piermarini, P.M., Choe, K.P., 2005. The multifunctional fish gill: dominant site of gas exchange, osmoregulation, acid-base regulation, and excretion of nitrogenous waste. Physiol. Rev. 85, 97–177.
Farrell, A.P., Sobin, S.S., Randall, D.J., Crosby, S., 1980. Intralamellar blood flow patterns in fish gills. Am. J. Physiol. Regul. Integr. Comp. Physiol. 239, R428–R436.
Froese, R., Pauly, D., 2007. Fishbase. http://www.fishbase.org/search.php. Accessed 5 Novembr 2019.
Giacomin, M., Schulte, P.M., Wood, C.M., 2017. Differential effects of temperature on oxygen consumption and branchial fluxes of urea, ammonia, and water in the dogfish shark (*Squalus acanthias suckleyi*). Physiol. Biochem. Zool. 90, 627–637.
Giacomin, M., Dal Pont, G., Eom, J., Schulte, P.M., Wood, C.M., 2019. The effects of salinity and hypoxia exposure on oxygen consumption, ventilation, diffusive water exchange and ionoregulation in the Pacific hagfish (*Eptatretus stoutii*). Comp. Biochem. Physiol. A. Mol. Integr. Physiol. 232, 47–59.
Giacomin, M., Onukwufor, J.O., Schulte, P.M., Wood, C.M., 2020. Ionoregulatory aspects of the hypoxia-induced osmorespiratory compromise in the euryhaline Atlantic killifish (*Fundulus heteroclitus*): the effects of salinity. J. Exp. Biol. Doi:101242/jeb.216309.
Glover, C.N., Bucking, C., Wood, C.M., 2013. The skin of fish as a transport epithelium: a review. J. Comp. Physiol. B. 183, 877–891.
Gonzalez, R.J., McDonald, D.G., 1992. The relationship between oxygen consumption and ion loss in a freshwater fish. J. Exp. Biol. 163, 317–332.
Gonzalez, R.J., McDonald, G.D., 1994. The relationship between oxygen uptake and ion loss in fsh from diverse habitats. J. Exp. Biol. 190, 95–108.
Hofmann, E.L., Butler, D.G., 1979. The effect of increased metabolic rate on renal function in the rainbow trout, *Salmo gairdneri*. J. Exp. Biol. 82, 11–23.
Holmes, W.N., Donaldson, E.M., 1969. The body compartments and the distribution of electrolytes. In: Hoar, W.S., Randall, D.J. (Eds.), Fish Physiology: Excretion, Ionic Regulation, and Metabolism. 1. Academic Press, London, pp. 1–89.
Isaia, J., 1972. Comparative effects of temperature on the sodium and water permeabilities of the gills of a stenohaline freshwater fish (*Carassius auratus*) and a stenohaline marine fish (*Serranus scriba*, *Serranus cabrilla*). J. Exp. Biol. 57, 359–366.
Isaia, J., 1984. Water and nonelectrolyte permeation. In: Hoar, W.S., Randall, D.J. (Eds.), Fish Physiology: Gills – Ion and Water Transfer. Part B 10. Academic Press, London, pp. 1–38.
LeBlanc, D.M., Wood, C.M., Fudge, D.S., Wright, P.A., 2010. A fish out of water: gill and skin remodeling promotes osmo- and ionoregulation in the mangrove killifish *Kryptolebias marmoratus*. Physiol. Biochem. Zool. 83, 932–949.
Loretz, A.C., 1979. Water exchange across fish gills: the significance of triated-water flux measurements. J. Exp. Biol. 79, 147–162.
Madsen, S.S., Engelund, M.B., Cutler, C.P., 2015. Water transport and functional dynamics of aquaporins in osmoregulatory organs of fishes. Biol. Bull. 229, 70–92.
Mandic, M., Sloman, K.A., Richards, J.G., 2009a. Escaping to the surface: a phylogenetically independent analysis of hypoxia-induced respiratory behaviors in sculpins. Physiol. Biochem. Zool. 82, 730–738.
Mandic, M., Todgham, A.E., Richards, J.G., 2009b. Mechanisms and evolution of hypoxia tolerance in fish. Proc. R. Soc. B 276, 735–744.
Mandic, M., Speers-Roesch, B., Richards, J.G., 2013. Hypoxia tolerance in sculpins is associated with high anaerobic enzyme activity in brain but not in liver or muscle. Physiol. Biochem. Zool. 86, 92–105.
Martin, K.L.M., Bridges, C.R., 1999. Respiration in water and air. In: Horn, M.H., Martin, K.L.M., Chotkowski, M.A. (Eds.), Intertidal Fishes: Life in Two Worlds. Academic Press, London, pp. 54–78.
Matey, V., Iftikar, F.I., De Boeck, G., Scott, G.R., Sloman, K.A., Almeida-Val, V.M.F., Val, A.L., Wood, C.M., 2011. Gill morphology and acute hypoxia: responses of mitochondria-rich, pavement, and mucous cells in two species with very different approaches to the osmo-respiratory compromise, the Amazonian oscar (*Astronotus ocellatus*) and the rainbow trout (*Oncorhynchus mykiss*). Can. J. Zool. 89, 307–324.
Motais, R., Isaia, J., 1972. Temperature-dependence of permeability to water and to sodium of the gill epithelium of the eel *Anguilla anguilla*. J. Exp. Biol. 56, 587–600.
Nikinmaa, M., 1990. Vertebrate red blood cells. In: Bradshaw, S.D., Burrgren, W., Heller, H.C., Ishii, S., Langer, H., Neuweiler, G., Randall, D.J. (Eds.), Zoophysiology. 28. Springer-Verlag, Berlin, pp. 1–262.
Nikinmaa, M., Salama, A., 1998. Oxygen transport in fish. In: Perry, S.F., Tufts, B.L. (Eds.), Fish Physiology. 17. Academic Press, London, pp. 141–184.
Nilsson, G.E., 2007. Gill remodeling in fish - a new fashion or an ancient secret? J. Exp. Biol. 210, 2403–2409.
Olson, K.R., 1992. Blood and extracellular fluid volume regulation: Role of the renin-angiotensin system, Kallikrein-Kinin system, and atrial natriuretic peptides. In: Hoar, W.S., Randall, D.J., Farrell, A.P. (Eds.), Fish Physiology: The Cardiovascular System. Part B 12. Academic Press, London, pp. 135–254.
Onukwufor, J.O., Wood, C.M., 2018. The osmorespiratory compromise in rainbow trout (*Oncorhynchus mykiss*): the effects of fish size, hypoxia, temperature and strenuous exercise on gill diffusive water fluxes and sodium net loss rates. Comp. Biochem. Physiol. A. Mol. Integr. Physiol. 219-220, 10–18.
Onukwufor, J.O., Wood, C.M., 2020. Reverse translation: effects of acclimation temperature and acute temperature challenges on oxygen consumption, diffusive water flux, net sodium loss rates, Q_{10} values and mass scaling coefficients in the rainbow trout (*Oncorhynchus mykiss*). J. Comp. Physiol. B. 190, 205–217.
Perry, S.F., Jonz, M.G., Gilmour, K.M., 2009. Oxygen sensing and the hypoxic ventilatory response. In: Richards, J.G., Farrell, A.P., Brauner, C.J. (Eds.), Fish Physiology: Hypoxia. 27. Academic Press, London, pp. 193–253.
Postlethwaite, E.K., McDonald, D.G., 1995. Mechanisms of Na^+ and Cl^- regulation in freshwater-adapted rainbow trout (*Oncorhynhus mykiss*) during exercise and stress. J. Exp. Biol. 198, 295–304.
R Core Team, 2020. R: a language and environment for statistical computing. R Foundation for Statistical Computing, Vienna, Austria (Accessed 30 Apr 2020).
Randall, D.J., Daxboeck, C., 1984. Oxygen and carbon-dioxide transfer across fish gills. In: Hoar, W.S., Randall, D.J. (Eds.), Fish Physiology: Gills - Anatomy, Gas Transfer, and Acid-Base Regulation. Part A 10. Academic Press, London, pp. 263–314.
Randall, D.J., Baumgarten, D., Malyusz, M., 1972. The relationship between gas and ion transfer across the gills of fishes. Comp. Biochem. Physiol. 41A, 629–637.
Richards, J.G., 2011. Physiological, behavioral and biochemical adaptations of intertidal fishes to hypoxia. J. Exp. Biol. 214, 191–199.
Robertson, L.M., Kochhann, D., Bianchini, A., Matey, V., Almeida-Val, V.F., Val, A.L., Wood, C.M., 2015. Gill paracellular permeability and the osmorespiratory compromise during exercise in the hypoxia-tolerant Amazonian oscar (*Astronotus ocellatus*). J. Comp. Physiol. B. 185, 741–754.
Ruhr, I.M., Wood, C.M., Schauer, K.L., Wang, Y., Mager, E.M., Stanton, B., Grosell, M., 2020. Is Aquaporin-3 involved in water-permeability changes in the killifish during hypoxia and normoxic recovery in freshwater or seawater? J. Exp. Zool. https://doi.org/10.1002/jez.2393.
Scott, G.R., Wood, C.M., Sloman, K.A., Iftikar, F.I., De Boeck, G., Almeida-Val, V.M.F., Val, A.L., 2008. Respiratory responses to progressive hypoxia in the Amazonian oscar, *Astronotus ocellatus*. Resp. Physiol. Neurobiol. 162, 109–116.
Sinclair, B.J., Marshall, K.E., Sewell, M.A., Levesque, D.L., Willett, C.S., Slotsbo, S., Dong, Y., Harley, C.D.G., Marshall, D.J., Helmuth, B.S., Huey, R.B., 2016. Can we predict ectotherm responses to climate change using thermal performance curves and body temperature? Ecol. Lett. 19, 1372–1385.
Sloman, K.A., Mandic, M., Todgham, A.E., Fangue, N.A., Subrt, P., Richards, J.G., 2008. The response of the tidepool sculpin, *Oligocottus maculosus*, to hypoxia in laboratory, mesocosm and field environments. Comp. Biochem. Physiol. A. Mol. Integr. Physiol. 149, 284–292.
Soivio, A., Tuurala, H., 1981. Structural and circulatory responses to hypoxia in the secondary lamellae of *Salmo gairdneri* gills at two temperatures. J. Comp. Physiol. 145, 37–43.
Speers-Roesch, B., Mandic, M., Groom, D.J.E., Richards, J.G., 2013. Critical oxygen tensions as predictors of hypoxia tolerance and tissue metabolic responses during hypoxia exposure in fishes. J. Exp. Mar. Biol. Ecol. 449, 239–249. https://doi.org/10.1016/j.jembe.2013.10.006.
Stevens, E.D., 1972. Change in body weight caused by handling and exercise in fish. J. Fish. Res. Board Can. 29, 202–203.
Wood, C.M., Randall, D.J., 1973. The influence of swimming activity on water balance in the rainbow trout (*Salmo gairdneri*). J. Comp. Physiol. 82, 257–276.
Wood, C.M., Iftikar, F.I., Scott, G.R., De Boeck, G., Sloman, K.A., Matey, V., Valdez Domingos, F.X., Duarte, R.M., Almeida-Val, V.M.F., Val, A.L., 2009. Regulation of gill transcellular permeability and renal function during acute hypoxia in the Amazonian oscar (*Astronotus ocellatus*): new angles to the osmorespiratory compromise. J. Exp.

Biol. 212, 1949–1964.
Wood, C.M., Ruhr, I.M., Schauer, K.L., Wang, Y., Mager, E.M., McDonald, M.D., Stanton, B., Grosell, M., 2019. The osmorespiratory compromise in the euryhaline killifish: water regulation during hypoxia. J. Exp. Biol. 222, 204818. https://doi.org/10.1242/jeb.204818.
Wright, P.A., Pärt, P., Wood, C.M., 1995. Ammonia and urea excretion in the tidepool sculpin *Oligocottus maculosus*: sites of excretion, effects of reduced salinity and mechanisms of urea transport. Fish Physiol. Biochem. 19, 111–123.
Yoshiyama, R.M., Valey, C.J., Schalk, L.L., Oswald, N.M., Vaness, K.K., Lauritzen, D., Limm, M., 1995. Differential propensities for aerial emergence in intertidal sculpins (Teleostei; Cottidae). J. Exp. Mar. Biol. Ecol. 191, 195–207.